Indian Journal of Chemical Technology
Vol. 29, November 2022, pp. 737-744
DOI: 10.56042/ijct.v29i6.

Synthesis and characterization of Fe_2O_3 nanoparticles incorporated PVA nanocompositefilms

J Satheesh Goud*,[1] & N Narsimlu[2]

[1]Telangana Tribal Welfare Residential Degree College (Men), Maripeda, Mahabubabad, 506 315, Telangana, India

[1,2]Department of Physics,Osmania University, Hyderabad, 506 007, India

E-mail: sg.jalagam@gmail.com

Received: *19 August 2022; accepted*: *21 October 2022*

Polyvinyl alcohol–iron oxide nanocomposite (PVA-Fe_2O_3 NC) films have been formed when iron oxide nanoparticles (Fe_2O_3 NPs) are incorporated into a polyvinyl alcohol (PVA) base matrix. In this study, for the preparation of a series of PVA-Fe_2O_3 NC films, different weight percentages (0, 2, 4, 6, and 8 wt. %) of Fe_2O_3 NPs have been added into the PVA solution using the solution cast method. The morphological and spectroscopic properties of the PVA-Fe_2O_3 NC films have been studied using X-ray diffraction (XRD), scanning electron microscopy (SEM), and ultraviolet-visible spectrophotometry (UV-Vis) spectroscopy techniques. XRD studies reveal that the original structure of the Fe_2O_3 NPs is preserved in the PVA-Fe_2O_3 NC films, and the crystallinity of the PVA-Fe_2O_3NC films has been increased. The SEM images confirm that the Fe_2O_3 NPs have been homogeneously distributed in 3-dimension with dots and rod-like structures. The UV-visible investigations have been carried out for the series of PVA-Fe_2O_3 NC films, which result in a significant change in opto-electronic properties. With an increasing weight percentage of Fe_2O_3 NPs in the PVA-Fe_2O_3 NC films, the direct bandgap decreased from 5.39 eV to 5.01 eV, the indirect bandgap decreased from 4.73 eV to 3.27 eV, the Urbach energy increased from 0.428 eV to 0.538 eV, the linear refractive index increased from 1.63 to 5.86, and the extinction coefficient increased from 1.86 X 10^{-6} to 1.74 X 10^{-5}. These results have shown that the spectroscopic properties of PVA-Fe_2O_3 NC films are modified considerably with the small addition of Fe_2O_3 NPs in the PVA matrix, which are useful for optoelectronic applications.

Keywords: Iron oxide (Fe_2O_3), Nanocomposite film, Optical conductivity, Polyvinyl alcohol (PVA), Refractive index

Recent studies of nanocomposite materials have shown that the polymers doped with nanoparticleshave improved their performance[1-7]. The main causes of this improvement in the nanocomposite materials are their small size, large surface area, quantum confinement effects, and strong interfacial interactions[8-12]. Out of many polymers, polyvinyl alcohol (PVA) is a well-known water soluble, non-toxic, biocompatible, biodegradable, environmentally friendly, semi crystalline, good interfacial interacting, good film-forming, cost-effective polymer[13,14]. PVA has special properties like high optical transparency and good dielectric strength. The properties of PVAdepend on the nature and percentage of dependent material. These properties are mainly due to the alkyl groups (OH) present in PVA, which form hydrogen bonds with the dopant[15]. When metal oxide nanoparticles are doped with PVA, the interaction may be in the form of hydrogen bonding with the metal oxide nanoparticles[16]. PVA is mostly used in bio-medical applications, including tissue engineering, contact lenses, artificial organs, orthopaedic materials, pharmaceuticals, packaging, and optoelectronic applications[13-16].

Fe_2O_3 NPs have special properties like good electron mobility, magnetic ability, and a 2.2 eV optical energy bandgap, which are useful for optoelectronic applications.Fe_2O_3 NPs have potential applications in the fields of medicine, life sciences and computer technology like Magnetic Resonance Imaging (MRI), drug carriers in delivery, gene carriers in gene therapy, nanofertilizers, non-fungicides, nanopesticides, nanofood, food packing, nanocoating, nanosensors, nanoscale memory, nanowires, spintronics etc. They can be used as filters in sunscreens, biosensors[17-19].

In this article, the PVA-Fe_2O_3NC films were synthesizedusing the solution casting technique, and their characteristics were studied using morphological and spectroscopic methods. In the UV-Visible spectra of the PVA-Fe_2O_3NC films, with increasing Fe_2O_3 NPs wt.%, absorption was increased in the UV wavelength region. This property of UV absorption by PVA-Fe_2O_3 NC films is useful to protect us from harmful UV

radiation from solar light. Thus, the PVA-Fe_2O_3 NC films can be used as UV-filters to protect us from skin diseases.

Experimental Section

Materials used

Polyvinyl alcohol (PVA) is bought from S D Fine-chem Limited (SDFCL). Its molecular weight is specified as M.W.: 85,000-1,24,000.The Fe_2O_3 NPs were purchased from Ad-nano Technologies Pvt. Ltd., Bangalore. Thespecificationsgiven on that arepurity: 99.9%, molecular formula: Fe_2O_3, the average Fe_2O_3NP size:30-60 nm, molecular weight:159.69 g/mol, melting point:1,565°C, physical form: powder, morphology: spherical, and red in colour. Petri dishes were purchased from Polylab.

Synthesis of PVA-Fe_2O_3 NC films

A clean and dry beaker witha volume capacity of 100 ml was taken. It is filled with distilled water up to the 80mL mark. 3g of PVAwas mixedin that water.The mixture was stirred well on a magnetic stirring machine at a speed of 600 rotations per minute (RPM) for six hours.The mixture turned into asolution of transparent homogenous viscous gel.

The gel was poured into the Petri dishes to form a film with a thickness of about 60µm. It was allowed to dry to form a dry film of pure PVA.The same process was repeated by addingFe_2O_3 NPs of different weight percentages to the pure PVA gel. The different weight percentages of Fe_2O_3 NPs (2wt.%, 4wt.%, 6wt.%, and 8wt.%) of 3g of PVA were dissolved in water before being mixed with the PVA solution separately. Those mixtures were magnetically stirred well again at a speed of 600 RPM for 6 h to get better dispersion of Fe_2O_3 NPs in PVA gel. The process of mixing is minimized the formation of agglomeration. The solutions were turned a reddish colour due to iron oxide. Those uniformly thick solutions were transferred into Petri dishes separately to form films of a thickness of about 60µm each using solvent cast technology[20]. They were allowed to dry at room temperature until films were formed. It took 30 days for the formation of films in our laboratory. As shown in Fig. 1, the films were removed from the Petri dishes and cut into rectangular pieces of suitable sizes for the study of their characterization.

Characterization techniques used

For morphology studies of PVA-Fe_2O_3 NC films, an X-ray diffractometer (SHIMADZU XRD-7000) having an X-ray tube holding Cu-$K_\alpha$target was used. It has40.0 kV accelerating voltage and a 30.0 mA operating current for its operation. The X-ray diffraction measurement was taken at the scattering angle (2θ), rangingfrom 10°to 80°, andat a wavelength of 0.15406 nm.XRD has been taken to investigate the existence of the crystalline nature of pure PVA and PVA-Fe_2O_3NCmaterial. For the surface morphological images, SEM images were obtained by using an FEI Quanta-250 SEM coupled device with X-ray detectors at 10kV.The UV-visible absorption data was obtained by a spectrometer (SHIMADZU UV–1800 series) in the 190-1100 nm wavelength range.

Results and Discussion

The results obtained from XRD, SEM images, and UV visible spectra wereanalyzedand discussed.

XRD Analysis

From the peaks of the XRD graph of PVA + x wt.% Fe_2O_3(x=0, 2, 4, 6, and 8), the results were analysed.Figure 2 shows the XRD graph of pure PVA (0 wt.% Fe_2O_3) and PVA+2 wt.%Fe_2O_3 NC films. The curves have intense peaks located at 19.8°with a large width to confirm the semi-crystalline nature of PVA films[20].The two peaks observed at 41.8° and 63.86° for PVA+2 wt.% Fe_2O_3 NC film are matched with JCPDS card No. 39-1346, which confirms the presence of

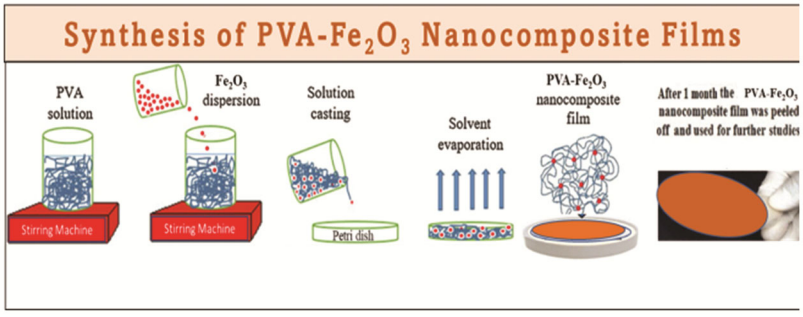

Fig. 1 — Synthesis of PVA-Fe_2O_3 NC film.

Fe_2O_3 NPs in the sample. It leads to the existence of the crystalline nature of the PVA-Fe_2O_3NC material[21,22]. Hence, by the addition of Fe_2O_3NPs in PVA, the crystallinity of the PVA-Fe_2O_3NC material is improved.

SEM images

The surface morphology of the PVA-Fe_2O_3 NC films can be determined by the SEM images. The SEM image of pure PVA is shown in Fig. 3(a), which is a smooth, homogeneous surface with a tight package. The SEM images of 4wt%, 6wt.%, and 8wt.% of PVA-Fe_2O_3 NC films are shown in Fig. 3(b), (c), and (d) respectively. The films have relatively rough surfaces with homogeneously distributed Fe_2O_3NPs in a zig-zag pattern with dots and rod-like structures in three dimensions. The property of larger surface area

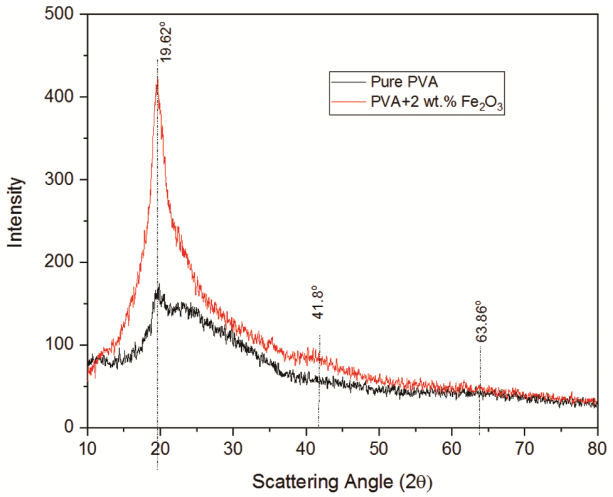

Fig. 2—XRD analysis of pure PVA and PVA+2wt.% Fe_2O_3 NC film.

nanofiller of Fe_2O_3NPs can be used as a gas sensor in gas sensing devices[7]. The hydrogen bonds are responsible for the interaction between Fe_2O_3NPs and PVA. These hydrogen bonds are formed when Fe_2O_3NPs are surrounded by OH groups of PVA. There are a few large, intense, white-coloured particles seen due to the formation of agglomeration by PVA chain molecules[23].

UV-Visible spectra

From the data of UV-visible absorbance spectra, optical energy band gap, refractive index, optical dielectric, and optical conductivity of PVA-Fe_2O_3 NC films can be calculated for better analysis.

UV-vis absorption spectra

In Fig. 4 the UV-visible absorbance spectra of PVA-Fe_2O_3NC films can be seen. The spectrum shows a high absorption edge at a wavelength of 191 nm in the lower wavelength of UV region, and for the wavelengths above 400 nm, the absorption of each film is almost constant and nearer to zero[20]. The UV absorbance values of PVA-Fe_2O_3NC films were increased with increasing Fe_2O_3 NPs wt.% in the films, and the absorption edge also gradually moved towards higher wavelengths. At 250 nm, the characteristic absorption band of PVA can be observed, which is related to the $\pi \rightarrow \pi^*$electron transition[24]. At 343 nm, there is a poignant and small absorption band that can be observed as shown in Fig. 4 and its position did not change even when the Fe_2O_3wt.% was increased in the PVA-Fe_2O_3NC films. This observation confirms the dispersion of theFe_2O_3NPs in the PVA matrix. The band energy corresponding to the characteristic

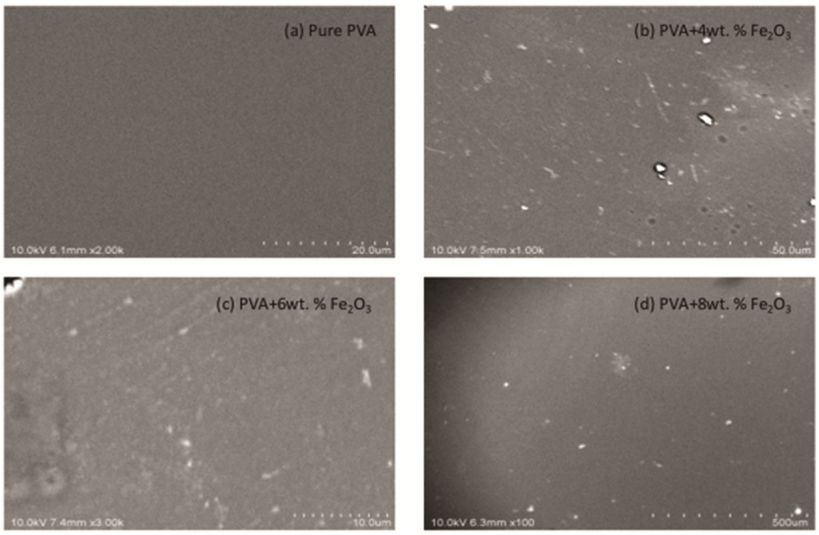

Fig. 3 — SEM images of (a) pure PVA, (b) PVA+4wt.%Fe_2O_3, (c) PVA+6wt.%Fe_2O_3, and (d) PVA+8wt.%Fe_2O_3 NC films.

absorption band at 343 nm of PVA will be 3.62 eV, which lies in between the optical band gap energy of pristine Fe_2O_3 (2.2 eV) and pristine PVA (6.27eV). This property of variation of the energy band gap of the PVA-Fe_2O_3 NC material is suitable for the preparation of optoelectronic devices such as tuneable photosensors[24]. Over exposure to UV radiation can cause severe negative effects on human health, like skin diseases and cancer[25].

In UV-Visible spectra, with increasing Fe_2O_3 NPs wt.% in PVA-Fe_2O_3NC films, the absorption in the UV region increased. Hence, PVA-Fe_2O_3NC material can be used as UV filters to protect us from harmful UV rays.

Optical energy direct and indirect band gap

The optical behaviour of PVA-Fe_2O_3NCmaterials can be determined by optical energy band gap, Urbach energy, refractive index, optical dielectric, and optical conductivity. The optical energy band gap can be calculated using the absorption coefficient (α). The absorption coefficient (α) is defined as the measure of the capacity of a material to absorb the amount of intensity of incident light per unit thickness of the sample. It can be determined using Beer Lambert's relation[24] given by

$$\alpha = \frac{(2.303*A)}{t} \quad \ldots (1)$$

where, A is the absorbance taken from the UV-Vis data. "A" is defined as the logarithmic ratio of the intensities of the incident beam to the transmitted beam$A = \log\left(\frac{I_o}{I}\right)$ and"t" is the thickness of the PVA-Fe_2O_3NC film samples. The t values of the analysed samples were measured with a screw gauge. They were 0.0052, 0.0052, 0.0062, 0.0058, and 0.0067 cm for the PVA-Fe_2O_3NC film samples containing 0, 2, 4, 6, and 8 wt.% of Fe_2O_3NPs, respectively. The Davis and Mott's relation[26] can be used to determine the optical energy band gap E_g value and is given by,

$$(\alpha h\nu)^m = \beta(h\nu - E_g) \quad \ldots(2)$$

Where $h\nu$ is the energy of the incident photon, β is a constant, and m is a variable having a value of 2 and 1/2, respectively, denoting the permitted direct and indirect transitions[27]. The direct energy band gap (E_{gd}) is calculated from the graph drawn between $(\alpha h\nu)^2$ versus energy$(h\nu)$ shown in the Fig. 5 and the indirect energy band gap (E_{gid}) is calculated from the graph drawn between $(\alpha h\nu)^{1/2}$ versus energy$(h\nu)$ as shown in the Fig. 6. The band gap energy values can be determined

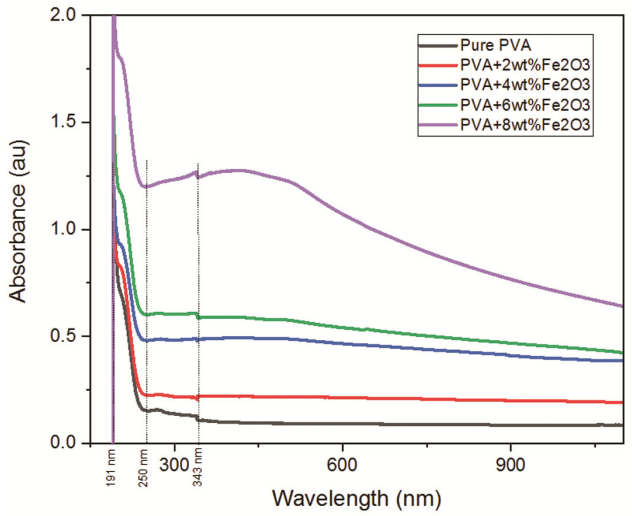

Fig. 4—Absorption spectra of PVA+ x wt.% Fe_2O_3 NC films for the varying x values.

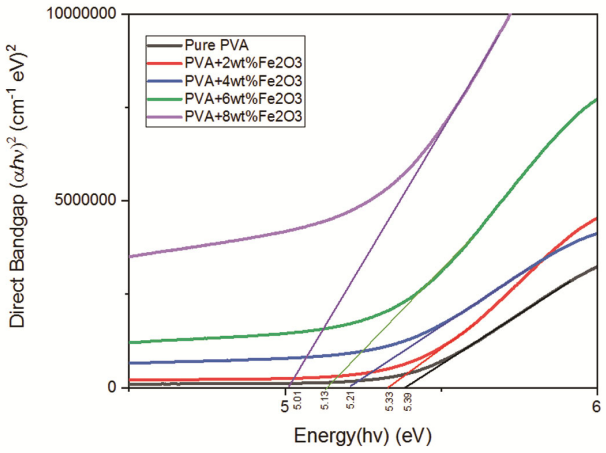

Fig. 5—Tauc plot of direct band gap versus PVA-Fe_2O_3 NC films.

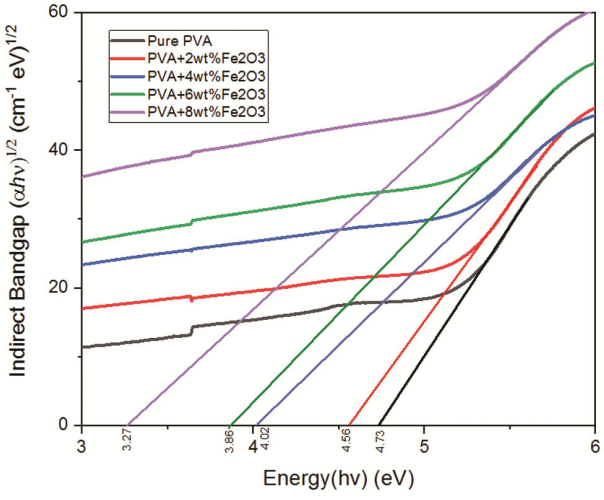

Fig. 6—Tauc plot of indirect band gap versus PVA-Fe_2O_3 NC films.

Table 1 — Optical energy Direct band gap, Indirect band gap, Urbach energy, Linear refractive index and Extinction coefficient of PVA- Fe2O3 NC films.

Composition PVA + x wt.% Fe_2O_3	Direct band gap E_{gd}(eV)	Indirect band gap E_{id} (eV)	Urbach energy E_u(eV)	Linear refractive index (n)	Extinction coefficient (k)
x = 0	5.39	4.73	0.370	1.64	0.00016
x = 2	5.33	4.56	0.490	2.08	0.00036
x = 4	5.21	4.02	0.894	1.96	0.00032
x = 6	5.13	3.86	0.901	2.35	0.00043
x = 8	5.01	3.27	1.543	2.67	0.00065

by extending the tangent drawn to the linear section up to the energy *(hv)* axis at zero value of absorbance[28]. The experimental values are tabulated in Table 1.

Urbach energy

For the confirmation of disorder present in the nanocomposite film, the Urbach energy (E_u) is determined. The Urbach energy (E_u) can be found from a plot drawn between the natural logarithmic value of absorption coefficient $ln(\alpha)$ and photon energy (hv), and then taking the reciprocal of the slope obtained by the linear part of the rising curve gives the value of the Urbach energy (E_u)[28]. The plot exhibited linear behaviour at the fundamental absorption edge, indicating that the PVA-Fe_2O_3NC materials obey the Urbach empirical relation[24,29]

$$\alpha = \alpha_o e^{(hv/E_u)} \quad \ldots(3)$$

The calculations showed that the E_u values were increased with the increasing addition of wt.% of Fe_2O_3NPs in the PVA-Fe_2O_3NC films.

Refractive index (n) and Extinction coefficient (k)

The complex refractive index of the PVA-Fe_2O_3 NC material is a function of the wavelength (λ) of the incident photons andis given by[30]

$$n^*(\lambda) = n(\lambda) + ik(\lambda) \quad \ldots(4)$$

where $n(\lambda)$ is the real part called the linear refractive index, and $k(\lambda)$ is the imaginary part called the extinction coefficient. The n and k parameters are considered for photo electronic applications[26]. The relation among linear refractive index *n,* extinction coefficient *k*, and reflectance *R* is given by[30]

$$n = \frac{1+R}{1-R} + \sqrt{\frac{4R}{1-R} - k^2} \quad \ldots(5)$$

The value of *k* is a measurement of the energy lost by an incident photon of UV radiation when it interacts with the free electrons present in the material[26]. The value of *k* can be calculated using the formula,

$$k = \frac{\alpha\lambda}{4\pi} \quad \ldots(6)$$

where α is absorption coefficient and λ is the wavelength of the UV light used.

For materials that have a very low value of extinction coefficient when compared with their linear refractive index($k \ll n$), the linear refractive index n reduces to[26]

$$n = \frac{1+\sqrt{R}}{1-\sqrt{R}} \quad \ldots(7)$$

The transmittance (T)of the PVA-Fe_2O_3NC materials can be calculated using the Beer-Lambert law[13,17], given by the relation

$$T(\%) = Antilog(2 - A), \text{or} T(\%) = 100 * 10^{-A} \quad \ldots(8)$$

Where, 'A' is the absorbance taken from the UV-visible spectra. Using the transmittance (T) value, the value of reflectance R of the PVA-Fe_2O_3NC materials can be determined using the relation[31]

$$R = 1 - (T * e^A)^{1/2} \quad \ldots(9)$$

A plot is drawn, taking the variation of linear refractive index (n)on the Y-axis and wavelength (λ) on the X-axis as shown in Fig.7. From this plot, then values suddenly fall in the UV region, meaning electronic transitions occurred there, and in the visible region the *n* values are almost static, meaning there is a normal dispersion of light energy taking place.

There is a variation in the linear refractive index (n) value of differentPVA-Fe_2O_3NC films, indicating that there will be different electronic transitions of the PVA-Fe_2O_3 NC film materials. Hence, the films have characteristic interactions with the propagating photons. With increasing Fe_2O_3 doping in PVA+*x* wt.% Fe_2O_3 (*x* = 0, 2, 4, 6, and 8), the refractive index

(n) value increased from 1.63 to 5.86 at a wavelength (λ) of 600 nm in the visible region. The refractive index (n) values taken from the plot are posted in Table 1 for future studies. This variation in the PVA-Fe_2O_3 NC materials can be used to prepare refractive index controlled optical devices[26].

The plot drawn taking extinction coefficient (k)on the Y-axis and wavelength (λ) on the X-axis is shown in Fig. 8. From the plot, there is a fall in$k$ values in the UV region below 250 nm, which confirms that incident photons have sufficient energy to raise the electronic transition to a higher energy level. Above 250 nm, which is in the higher UV and visible region, there is a rise in$k$ value, which confirms that incident photons have insufficient energy to raise the electron transition to a higher energy level[31]. Hence, there is alow loss of photon energy due to scattering or reflection by the PVA-Fe_2O_3NC films in the visible region, which makes them suitable for the fabrication of optoelectronic devices. From Fig. 8, it can be observed that with increasing addition of Fe_2O_3NPs with increment steps of 2 wt.% from 0 to 8 wt.% in the PVA-Fe_2O_3 NC films, the values of extinction coefficient k are increased. The extinction coefficient k values taken at a fixed wavelength (λ) of 600 nm in the visible region of the incident photons are increased from 1.86 × 10^{-6} to 1.74 × 10^{-5},and those values are tabulated in Table (1).

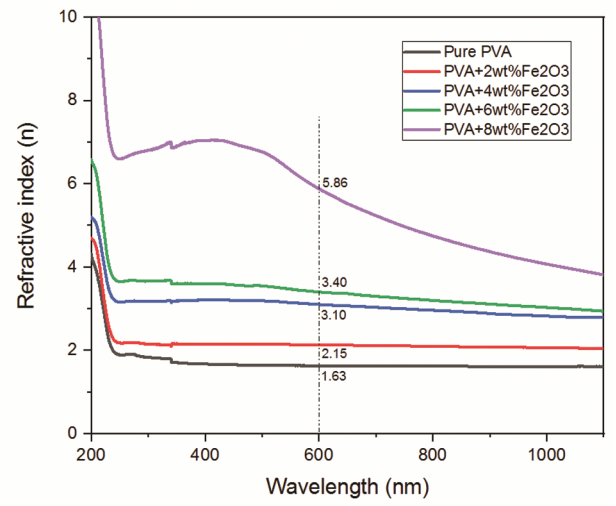

Fig. 7—Refractive index of PVA-Fe_2O_3 NC films.

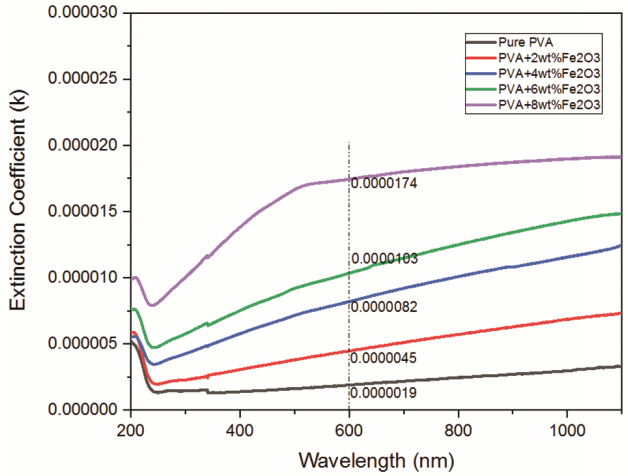

Fig. 8—Extinction coefficient of PVA-Fe_2O_3 NC films.

Optical dielectric constant

The optical complex dielectric constant depends on the linear refractive index(n) and the extinction coefficient (k) given by the relation

$$\varepsilon^* = \varepsilon' - i\varepsilon'' = (n^2 - k^2) - i(2nk) \quad \ldots(10)$$

Where the real part (ε') is the energy storage capacity of the material, and the imaginary part (ε'') is a measure of energy loss for the incident photons or absorbed energy through the dielectric field[32].

As shown in Fig. 9, the ε' value increased with increasing the wt.% of Fe_2O_3 NPs. The ε' value is low and almost constant up to 5 eV (248 nm) due to insufficient photon energy of the incident light, and beyond this value, the dielectric constant $\varepsilon'$is increased. There is a variation in the PVA+8wt.%Fe_2O_3 values due to the formation of agglomeration for the higher weight percentage of nanofiller. In the case of the imaginary dielectric constant (ε''), from Fig. 10, its value decreases up to 5 eV and then again increases beyond this value. It is the consequence of the variation of n and k values.

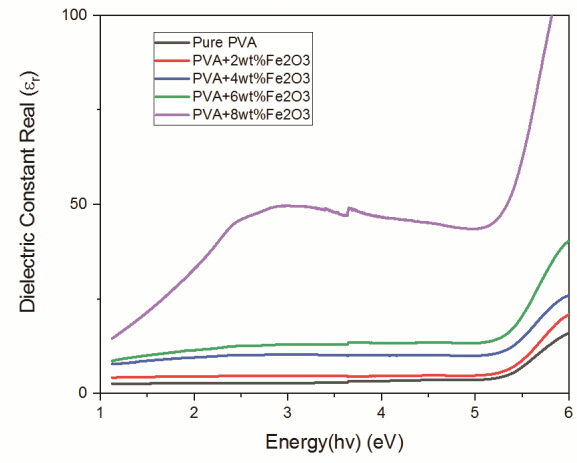

Fig. 9—Real part of tedielectric constant of PVA-Fe_2O_3 NC films.

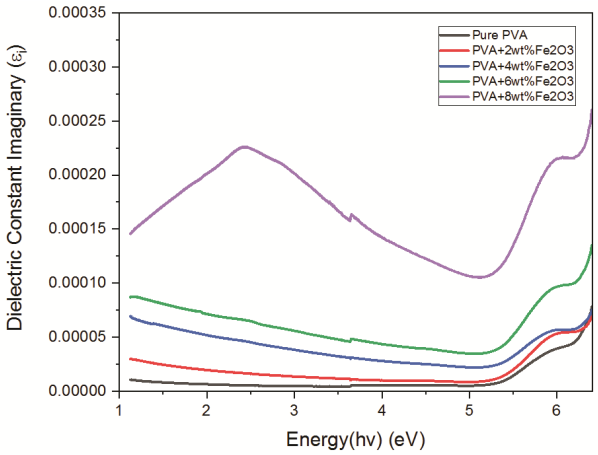

Fig. 10—Imaginary part of PVA-Fe_2O_3 NC films

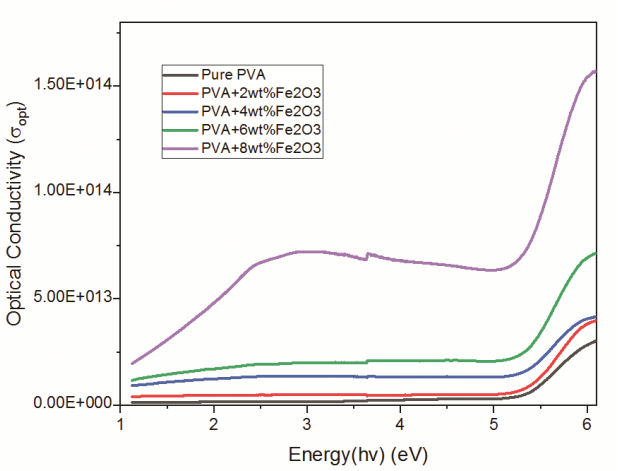

Fig. 11—Optical conductivity of Fe_2O_3 NC films.

Optical conductivity

The optical conductivity(σ_{opt})is due to the mobility of free charge carriers because of the excitation of electrons caused by incident photons. It depends on the linear refractive index (n), absorption coefficient (α)and speed of light (c) given by the equation[33]

$$\sigma_{opt} = n\alpha c/4\pi \quad \ldots(11)$$

The value of the speed of light(c) in vacuum is $3 \times 10^{10} cm/s$. The variation of optical conductivity (σ_{opt}) with the incident photon energy (hv)of PVA-Fe_2O_3 NC films is shown in Fig. 11. From the curves, it is observed that the optical conductivity (σ_{opt}) of the PVA-Fe_2O_3 NC films was greatly enhanced with increasing nanofiller weight percentage.

Conclusion

In this article, the morphological and optical properties of the PVA-Fe_2O_3NCfilm material have been discussed. It was observed that the dispersed Fe_2O_3NPs in PVA polymer have influenced the surface morphology, topography, optical band gap, and refractive index. The SEM images have confirmed that Fe_2O_3 NPs are homogeneously distributed in the PVA-Fe_2O_3NC film and Fe_2O_3 NPs have increased the roughness of the surface. This property of increasing surface area by the nanofiller of Fe_2O_3NP is useful in gas sensing devices. The UV-visible spectroscopic absorption graph has shown the characteristic absorption band energy of the PVA-Fe_2O_3NC film as 3.62 eV (343 nm), which is in between the optical band gap energy of pureFe_2O_3 (2.2 eV) and pristine PVA (6.27eV). This property of the material is suitable for the fabrication of optoelectronic devices like tuneable photosensors[21]. The results from the study have given a deeper understanding of how energy band gap decreases and disorder in the composite material increases with increasing Fe_2O_3 NP weight percentage in the PVA base matrix. The refractive index study has shown that there is an increase in the linear refractive index value with the rise of iron oxide weight percentage in the composite film, which is useful in the preparation of refractive index controlled optical devices. At a wavelength of 600 nm in the visible region, the variation of the extinction coefficient of the PVA-Fe_2O_3 NC film from 1.86×10^{-6} to 1.74×10^{-5} has revealed that there is low loss of photon energy in the visible region, which is suitable for the fabrication of optoelectronic devices. The results of the dielectric constant study have led to a deeper understanding of the variation of incident photon energy. The dielectric constant (ε') value increases with the increase in the addition of Fe_2O_3 NPs. The ε' value is low and almost constant up to 5 eV (248 nm) due to the insufficient photon energy of the incident light, and beyond this energy ε'value increases. The imaginary dielectric constant (ε'') value first decreases up to 5 eV and then again increases beyond this value. The optical conductivity (σ_{opt}) of the iron oxide nanocomposite films was greatly enhanced with increasing nanofiller weight percentage.

Acknowledgement

The authors are thankful to the Principal, Telangana Tribal Welfare Residential Degree College (Boys), Maripeda, and the Principal, University

College of Engineering (A), Osmania University, Hyderabad for providing the lab facility.

References

1 Murugan E, Santhoskumar S, Govindaraju S &Palanisamy M, *Spectrochim Acta A: Mol Biomol Spectrosc*, 246 (2021) 119036.
2 Santhoshkumar S & Murugan E, *Dalton Trans*, 50 (2021) 17988.
3 Murugan E & Jebaranjitham J N, *J Mol Catal A: Chem*, 365 (2012) 128.
4 Murugan E & Jebaranjitham J N, *Chem Eng J*, 259 (2015) 266.
5 Murugan E & Gopi V, *J Phys Chem C*, 115 (2011) 19897.
6 Murugan E, Jebaranjitham J N & Usha A, *Appl Nanosci*, 2 (2012) 211.
7 E Murugan, Rangasamy R & Jebaranjitham J N, *Adv Sci Lett*, 6 (2012) 250.
8 Murugan E & Dhomodharan A, *Diam Relat Mater*, 120 (2021) 108684.
9 Murugan E & Dhomodharan A, *Diam Relat Mater*, 128 (2022) 109268.
10 Kesava M & Dinakaran K, *Int J Hydrogen Energy*, 46 (2021) 1121.
11 Kesava M & Dinakaran K, *J Phys Chem C*, 125 (2020) 130.
12 Kesava M, Saravanan V, Srinivasan K & Dinakaran K, *Int J Energy Res*, 46 (2022) 18162.
13 Ahmed H & Zinah S H, *Egypt J Chem*, 63 (2020) 461.
14 Bulinski M, *Molecules*, 26 (2021) 2886.
15 Shady M, El-Dafrawy, Mahmoud T, Salem S & Shawky M H, *Sci Rep*, 11 (2021) 11404.
16 Ananya B, Ayan D & Mahuya D, J *Inorg Organomet Polym Mater*, 30 (2020) 2248.
17 Murugan E, Ariraman M, Rajendiran S, Kathirvel J, Akshata C R & Kumar K, *ACS Omega*, 3 (2018) 13685.
18 Nene A, Xuefeng Y, Poonam K, Hongrong L, Prakash S &Seeram R, *Material*, 13 (2020) 644.
19 Pulit-Prociak J, Krzysztof P, Jarosław C, Paweł S, Anita S, Elżbieta S, Sławomir M A & Marcin B, *J Inorg Organomet Polym Mater*, 29 (2019) 390.
20 Lalitha G, R Saravanan H R, Ravichandran K, Gracia F, Shilpi A & Vinod K G, *J Photochem Photobiol B: Biol*, 173 (2017) 43.
21 Omed G A, Shujahadeen B A, Mariwan A & Rasheed A, *Result Phys*, 6 (2016) 1006.
22 Huizang J, Quianquan Z, Xiaofeng L, Yongtai Y, Yan L & Yaming Z, *RSC Nanoscale Adv*, 2 (2020) 5296.
23 Restrepo I, Flores P & Rodríguez Llamazares S, *Polym Plast Technol Mater*, 58 (2019) 105.
24 Shobhana C & Sengwa R J, *Curr Appl Phys*, 2 (2018) 592.
25 Yang W, Jing S, Ting L, Piming M, Huiyu B, Yi X, Mingqing C &Weifu D, *ACS Appl Mater Interfaces*, 9 (2017) 36281.
26 Naresh K, Sengwa R J, Priyanka D & Mukul S, *Indian J Eng Mater Sci*, 29 (2022)169.
27 Rajeshwar R A, Ch S & Narsimlu N, *J Appl Phys*, 13 (2021) 45.
28 Satheesh Goud J & Narsimlu N, *J Appl Phys*, 13 (2021) 2278.
29 A Rajeshwar R A, Ashok B, Krishnamurthy G K, Aparna D, Ch. S & Narsimlu N, *Am J Eng Res*, 10 (2021) 105.
30 Prinyanka D & Sengwa R J, *Optik Int J Light Electron Optics*, 241 (2021) 167215.
31 Satheesh Goud J, Ch. S & Narsimlu N, *Mater Today,* 67-6 (2022) 872.
32 Abdel-Salam I A, Awad M M, Soliman T S & Khalid A, *J Alloys Compd*, 898 (2022) 162946.
33 Soliman T S, Vshivkov S A & Elkalashy Sh. I, *Opt Mater*, 107 (2020) 110037.